

Supporting Information

A Smartphone-Based Fourier Ptychographic Microscope Using the Display Screen for Illumination

Kyung Chul Lee,[†] Kyungwon Lee,[†] Jaewoo Jung,[†] Se Hee Lee,[‡] Donghyun Kim,[†] and Seung Ah Lee^{*,†}

[†]*School of Electrical and Electronic Engineering, Yonsei University, Seoul, 03722, South Korea*

[‡]*Department of Computer Science, Yonsei University, Seoul, 03722, South Korea*

E-mail: seungahlee@yonsei.ac.kr

Section 1. Instructions to building a smartphone-based Fourier ptychographic microscope module

Table S1: List of the off-the-shelf components for our smartphone-based Fourier ptychographic microscope. The 3D-print design for the microscope module is included in section 4. (FL, focal length; Dia., diameter)

Off-the-shelf component	Quantity	Purpose	Suppliers and manufacturers
Google Pixel 3 XL smartphone (~\$400)	1	Image capture, <i>in-situ</i> calculation, and illumination with organic LED display	Amazon
X-Y movable stage caliper (~\$15)	1	Focusing stage	Amazon, AliExpress
3D-printed module (~\$150)	1	Housing for optical element and sample mount	Design included in Section 4
M12 imaging lens, 17.5 mm FL f/5.6 (~\$120)	1	Objective lens	Edmund Optics
Achromatic lens, 25 mm Dia. 125 mm FL (~\$96)	1	Tube lens	Edmund Optics
Achromatic lens, 20 mm Dia. 25 mm FL (~\$86.5)	1	Field lens	Edmund Optics
Achromatic lens, 18 mm Dia. 22.5 mm FL (~\$80)	1	Eyepiece	Edmund Optics
Ø1" round protected aluminum mirror (~\$15)	2	Optical path rotation	Thorlabs
Filter holder (Thorlabs, FH2) (~\$21)	1	Sample mount	Thorlabs
16-mm long M6 screws and nuts	5	Fix a main case	Thorlabs
10-mm long M2 screws	2	Attaching the focusing stage to the 3D printed module	Multiple suppliers (e.g. DigiKey)
10-mm, 16-mm long M3 screws	2	Attaching the focusing stage to the sample mount	Multiple suppliers (e.g. DigiKey)

Our smartphone-based Fourier ptychographic microscope is composed of off-the-shelf components and 3D printed parts as presented in Table S1. Once the housing is printed, users can easily assemble and turn their smartphone into a compact microscope. Figure S1 shows the final assembled result of our components. The overall size of the microscope

module is $9 \times 11 \times 11$ cm, and it weighs 400 g without the smartphone.

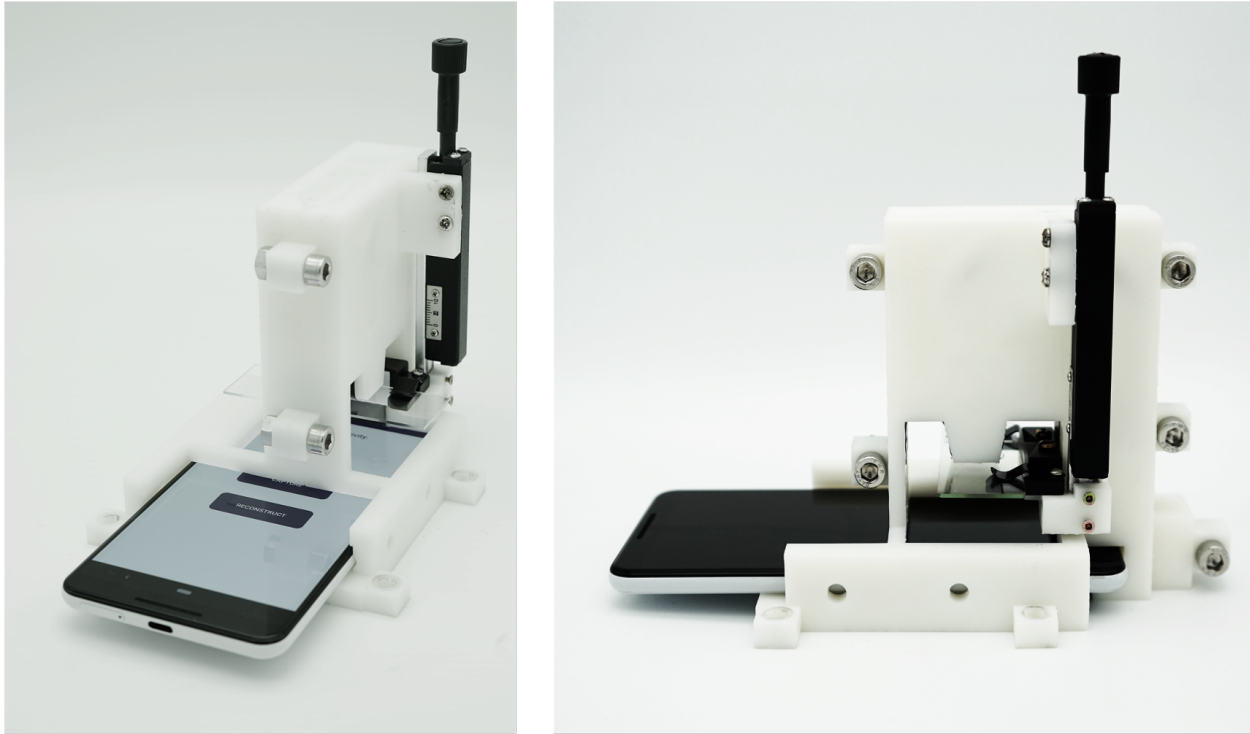


Figure S1: The assembled microscope module with a smartphone.

The main microscope housing

The 3D-printed main housing, which holds all optical elements and the smartphone in place, is designed with *Fusion 360* software based on the Zemax design of the microscope. We added $100 \mu\text{m}$ margin to the optics mount, accounting for the resolution of the 3D printer we used (*Formlabs Form 2*). The main housing is divided into two parts which are printed separately. To form a microscope unit, the optical components first need to be mounted and the divided parts are combined and tightened at five screw holes as shown in Figure S1.

Sample stage

A low-cost mechanical stage with a sample holder is mounted on the side of the main housing and is used to focus the microscope. We designed and 3D-printed a side arm connector to fix the sample stage on the microscope's main housing as presented in Figure S4. For imaging,

users can load a sample slide on the holder and adjust the focus of the microscope using the knob on the linear stage while viewing the preview image on the smartphone.

Assembly instructions

1. Print the main housing and the side arm module using a 3D printer. We recommend printing with an STL-type 3D printer using rigid resins.
2. Mount all optical elements including lens and mirrors on one side of the main housing as shown in Figure 2a. Join the opposite side and tighten the housing using M6 bolts and nuts to hold elements in place. (Figure S2b).

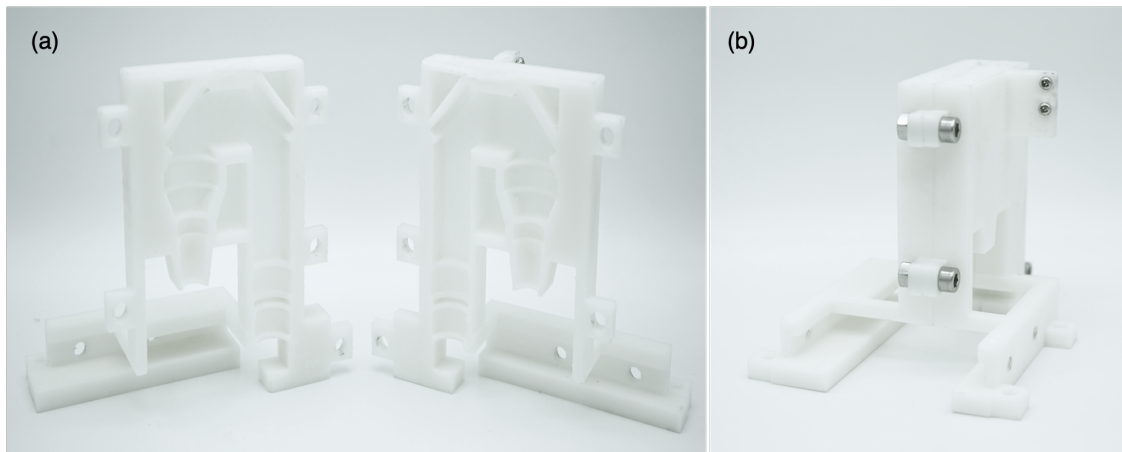


Figure S2: (a) 3D-printed main housing. (b) Main housing assembled with optical components.

3. Assemble the sample mount with the 3D-printed side arm connector and tight the screws indicated by the red circles in Figure S3.

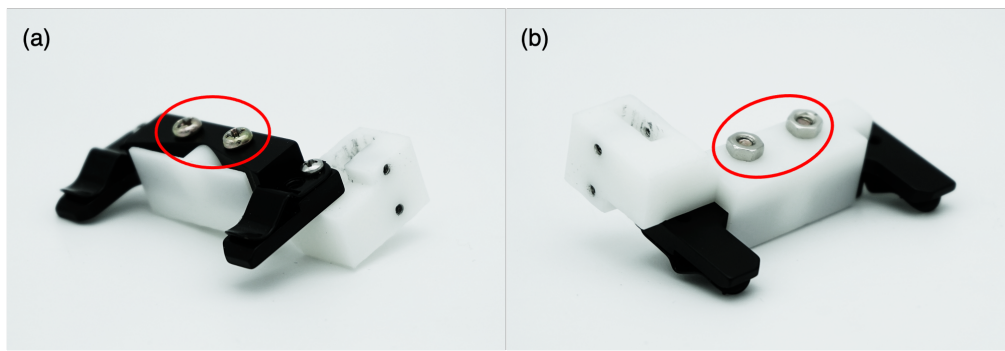


Figure S3: Assembled sample mount: (a) top view (b) bottom view.

4. Assemble the linear focusing stage with the side arm connector using two M2 screws (Figure S4).



Figure S4: Assembled sample stage.

5. Attach the assembled sample stage on the main case using two M3 screws. (Figure S5).



Figure S5: Sample stage connected to the main case.

6. Slide in the smartphone into the module to start imaging (Figure S6). The entire module can be fixed on the optical table using M6 screw holes on the bottom.



Figure S6: Fully assembled smartphone Fourier ptychographic microscope.

Section 2. Comparison of the reconstruction results between DNG and JPEG formats

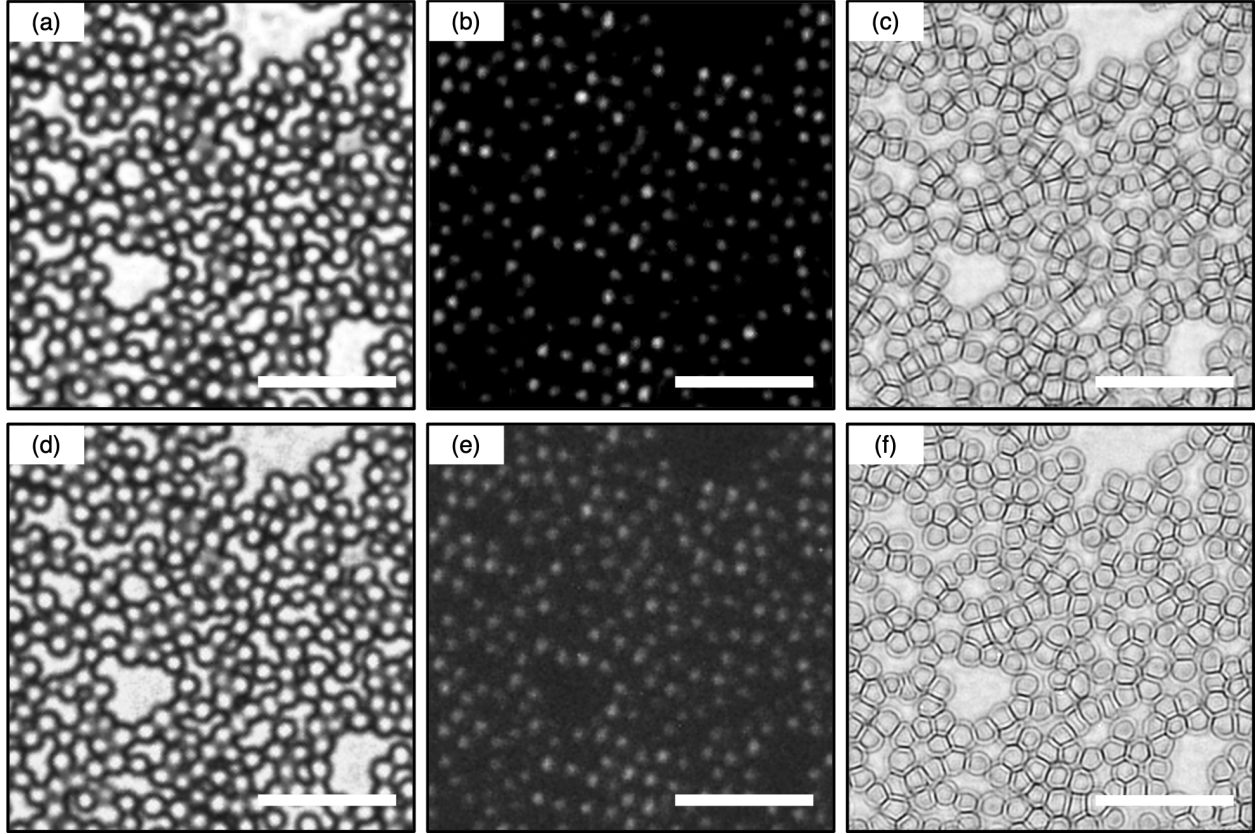


Figure S7: Top: JPEG-formatted raw images within the bright-field region (a) and dark-field region (b). (c) An FP reconstructed HR image using JPEG raw image sequences. Bottom: DNG-formatted raw images within the bright-field region (d) and dark-field region (e). (f) An FP reconstructed HR image using DNG-formatted raw image sequences. All scale bar is $50 \mu\text{m}$

The built-in camera for Google Pixel 3, which was utilized for our prototype, supports two saving formats for image files, namely, DNG and JPEG. The DNG format is the uncompressed, lossless raw image format supporting 10 bits per pixel, whereas the JPEG-formatted images are denoised and adjusted by the internal image processing pipeline of the camera and then compressed into 8-bit depth. Here a 2-bit of extended dynamic range in DNG format can be utilized to recover more accurate high-resolution (HR) complex fields, albeit this requires a greater loading time and additional Fourier Ptychography (FP) processing

time on the device. To determine which of the two data format should be used, we compared the quality of reconstructed amplitude of blood smear samples. While both the bright-field raw images (Figure S7a,d) show similar image quality, the DNG format of the dark-field raw image (Figure S7e) shows more details with a higher background level suggesting that denoising had been applied to the JPEG images. Meanwhile, no significant improvement can be observed in the reconstructed images (Figure S7c,f). A bit more detail in the boundaries of the red blood cells in the DNG-reconstructed image can be observed, while the hot pixels in the LR dark-field DNG images result in false bright spots in the reconstructed image. Based on this comparison, we decided to use the LR images in JPEG format, which has the advantages of rapid processing with a low data volume while ensuring comparable reconstruction quality.

Section 3. Comparison between monochromatic and color multiplexed illuminations

In many histological samples, staining and color imaging are used to highlight subcellular structures. For color FPM, there are two major approaches; sequential RGB capture and multiplexed capture. Programmable illumination with an organic LED screen is useful for adjusting the location and the brightness of color illuminations with 8-bit depth intensities of R, G, and B illuminations. Thus, smartphone-FPM can also utilize both sequential RGB illumination and the color multiplexing illumination approaches. The first approach is $3\times$ slower but we can adjust the exposure time of the camera for each color channel to achieve maximum SNR for all color channels. The second approach can be faster for image capture, but there may be issues coming from the demosaicing process since the bayer images are not available in smartphone FPM. Also, the screen's brightness and the image sensor's sensitivity vary across the color channels, and the screen's color pixel values need to be adjusted to capture all color channels with a single exposure time.

Figure S8 shows a monochromatic (green) reconstruction result using the monochromatic ($G = 255$) illuminated image sequence with a 300 ms exposure time (figure S8a) and the calibrated color ($R,G,B = 255, 117, 215$) illuminated image sequence with a 500 ms exposure time (figure S8b). While the signal intensity may be similar in both image sequences, the dark current noise in the multiplexed illumination is higher due to the longer exposure time. As a result, the calibrated color illuminated image shows a more noisy reconstruction result. To sum up, sequential RGB capture provides better reconstruction quality for the classic FPM on a smartphone where the image SNR is inherently limited.

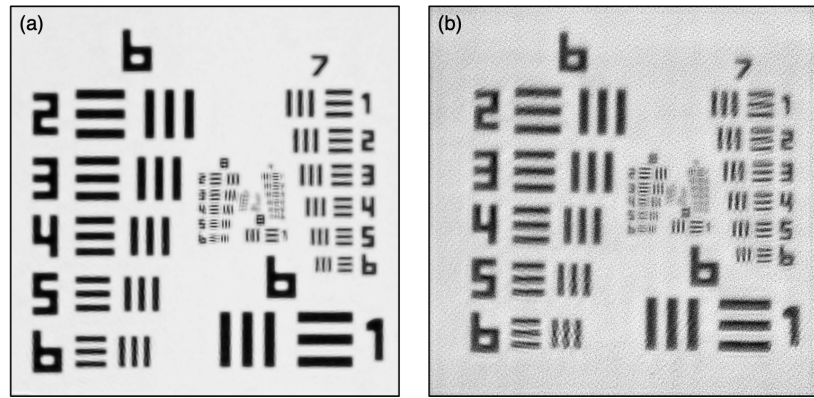


Figure S8: (a) Reconstruction result with monochromatic (green, 255) illumination and (b) calibrated color (red, 255; green, 117; blue, 215) illumination

Section 4. Comparison of the space-bandwidth product of smartphone-enabled microscopes

The space-bandwidth product (SBP) refers to the effective number of pixels required to represent an image and is a measure of the information content of the imaging system. This number is directly related to the diagnostic or screening capabilities of the microscope and can be calculated as follows:¹

$$SBP = \frac{FOV}{(0.5 \times \text{resolution})^2}$$

Table S2 presents the SBPs of previously reported portable smartphone microscopy devices implemented as an attachment to a smartphone or as hardware modules on which a smartphone is mounted. We excluded portable microscope designed with dedicated camera modules and microcomputers, or lens-less microscopes which require modification of the smartphone device.

The FOV of our system is 3.4 mm², which is the result of the effective pixel of 3000 × 2200 due to the distortion correction, and half-pitch resolution is 870 nm, which is measured in both center and edge of the FOV. Meanwhile, the FOV and the resolution reported in the previous works use various definitions but we selected the values in terms of the highest estimate. Our device achieves the SBP of 18 megapixels and exceeds the SBP of previous works by at least 30%.

Table S2: The SBPs of smartphone microscope implementations (BF, bright-field microscopy; DF, dark-field microscopy; PC, phase contrast; FM, fluorescence microscopy; PM, polarization microscopy)

Reference	FOV (mm ²)	Resolution (μm)	SBP (megapixels)	Modality	Resolution quantification method
Ours	3.4	0.87	18	BF,PC	measured half-pitch
Im et al., 2015 ²	14	2	14	PC	theoretical
Freeman et al., 2018 ³	2.5	0.87	13	BF	measured half-pitch
Zhu et al., 2019 ⁴	81	10	3.2	BF,FM,DF	measured half-pitch
Switz et al., 2019 ⁵	16	5	2.5	BF	measured half-pitch
Skandarajah et al., 2014 ⁶	0.52	1.74	0.68	BF,DF,PC	measured half-pitch
Wei et al., 2013 ⁷	0.36	1.5	0.64	FM	measured half-pitch
Pirnstill et al., 2015 ⁸	0.12	1.5	0.21	BF	measured half-pitch
Phillips et al., 2015 ⁹	0.16	2	0.16	BF,DF,PC	theoretical
Meng et al., 2017 ¹⁰	0.006	0.4	0.15	BF,PC	theoretical
Breslauer et al., 2009 ¹¹	0.025	1.2	0.07	BF,FM	size of the measured PSF
Jung et al., 2017 ¹²	0.069	2	0.07	BF,DF,PC	theoretical

Section 5. Reconstruction speed of the smartphone FPM

In our smartphone-FPM, the HR images can be reconstructed on the device. For each reconstruction, a region-of-interest (ROI) of 200×200 pixels is used, in order to consider and to correct for the spatially-varying pupil function of the microscope. In naive reconstruction mode, the app loads the entire LR image sequence in the smartphone's memory, selects the user-defined ROI, and performs the FP reconstruction. This process takes a total of 30 s, which includes 20 seconds for the loading of LR images (69 images) and 10 seconds for the actual FP reconstruction. Since the entire LR sequence is loaded on the memory of the smartphone, reconstruction of other ROIs can be performed right away, with the required computing time of 10 s per ROI. To reconstruct the full effective FOV of 3000×2200 pixels, a total 165 ROIs should be reconstructed. For a single ROI reconstruction, only 10% of the smartphone's CPU and the RAM is used; accordingly, there is a room for multi ROI process with parallel computing.

For faster reconstruction of the full FOV, the user can select the full FOV reconstruction mode in our application which utilizes parallel computing to process multiple ROIs at the same time. In this mode, five ROIs are computed in parallel and the total of 165 ROIs in the full FOV can be reconstructed in 845 seconds. Compared to the naive mode, this is roughly a factor of two faster for full-field. Also, if users want faster reconstruction, there is an option to send all data to the server, where the entire processing can be completed under 3 minutes including the file transfer time. The performance comparison is summarized in tableS3.

Table S3: Measurements of reconstruction time

	Single ROI reconstruction on a smartphone	Full FOV reconstruction on a smartphone	Full FOV reconstruction on a server
ROI size (raw image, pixels)	200 × 200	200 × 200	200 × 200
Full FOV size (raw image, pixels)	-	3000 × 2200	3000 × 2200
Number of ROIs	1	165	165
Output size (reconstructed amplitude & phase)	600 × 600 × 2	9000 × 6600 × 2	9000 × 6600 × 2
File I/O time (69 images)	20 s	20 s	120 s (file transfer time)
FP reconstruction time (69 images, 10 iterations)	10 s	825 s	30 s
Total time	30 s	845 s	150 s

* Benchmarked on a Google Pixel 3 XL with Qualcomm snapdragon 845 and a server with AMD Ryzen 3950X and RTX 2080ti GDDR6X

Section 6. Code availability

The STL 3D-print file for the microscope module and the customized Android application (in Kotlin) can be downloaded from http://github.com/OISL-Yonsei/Smartphone_FPM

References

- (1) Goodman, J. W. *Introduction to Fourier optics*; W.H. Freeman, 2017; pp 28–35.
- (2) Im, H.; Castro, C. M.; Shao, H.; Lioong, M.; Song, J.; Pathania, D.; Fexon, L.; Min, C.; Avila-Wallace, M.; Zurkiya, O., et al. Digital diffraction analysis enables low-cost molecular diagnostics on a smartphone. *Proceedings of the National Academy of Sciences* **2015**, *112*, 5613–5618.
- (3) Freeman, E. E.; Semeere, A.; Osman, H.; Peterson, G.; Rajadhyaksha, M.; González, S.; Martin, J. N.; Anderson, R. R.; Tearney, G. J.; Kang, D. Smartphone confocal microscopy for imaging cellular structures in human skin in vivo. *Biomedical Optics Express* **2018**, *9*, 1906–1915.
- (4) Zhu, W.; Pirovano, G.; Gong, C.; Kulkarni, N.; Nguyen, C. D.; Brand, C.; Reiner, T.; Kang, D. Smartphone-based epifluorescence microscope for fresh tissue imaging. European Conference on Biomedical Optics. 2019; p 11075_10.
- (5) Switz, N. A.; D'Ambrosio, M. V.; Fletcher, D. A. Low-cost mobile phone microscopy with a reversed mobile phone camera lens. *PLoS ONE* **2014**, *9*, e95330.
- (6) Skandarajah, A.; Reber, C. D.; Switz, N. A.; Fletcher, D. A. Quantitative imaging with a mobile phone microscope. *PLoS ONE* **2014**, *9*, e96906.
- (7) Wei, Q.; Qi, H.; Luo, W.; Tseng, D.; Ki, S. J.; Wan, Z.; Gorocs, Z.; Bentolila, L. A.; Wu, T.-T.; Sun, R., et al. Fluorescent imaging of single nanoparticles and viruses on a smart phone. *ACS Nano* **2013**, *7*, 9147–9155.

- (8) Pirnstill, C. W.; Coté, G. L. Malaria diagnosis using a mobile phone polarized microscope. *Scientific Reports* **2015**, *5*, 1–13.
- (9) Phillips, Z. F.; D'Ambrosio, M. V.; Tian, L.; Rulison, J. J.; Patel, H. S.; Sadras, N.; Gande, A. V.; Switz, N. A.; Fletcher, D. A.; Waller, L. Multi-contrast imaging and digital refocusing on a mobile microscope with a domed led array. *PLoS ONE* **2015**, *10*, e0124938.
- (10) Meng, X.; Huang, H.; Yan, K.; Tian, X.; Yu, W.; Cui, H.; Kong, Y.; Xue, L.; Liu, C.; Wang, S. Smartphone based hand-held quantitative phase microscope using the transport of intensity equation method. *Lab on a Chip* **2017**, *17*, 104–109.
- (11) Breslauer, D. N.; Maamari, R. N.; Switz, N. A.; Lam, W. A.; Fletcher, D. A. Mobile phone based clinical microscopy for global health applications. *PLoS ONE* **2009**, *4*, e6320.
- (12) Jung, D.; Choi, J.-H.; Kim, S.; Ryu, S.; Lee, W.; Lee, J.-S.; Joo, C. Smartphone-based multi-contrast microscope using color-multiplexed illumination. *Scientific Reports* **2017**, *7*, 1–10.